Reviews
doi.org/10.1002/batt.202000038

Chemistry Europe
European Chemical Societies Publishing

Recent Progress in Calix[*n*]quinone ($n = 4, 6$) and Pillar[5]quinone Electrodes for Secondary Rechargeable Batteries

Meng Zhang,[a] Yi Zhang,[a] Weiwei Huang,*[a, b] and Qichun Zhang*[b]

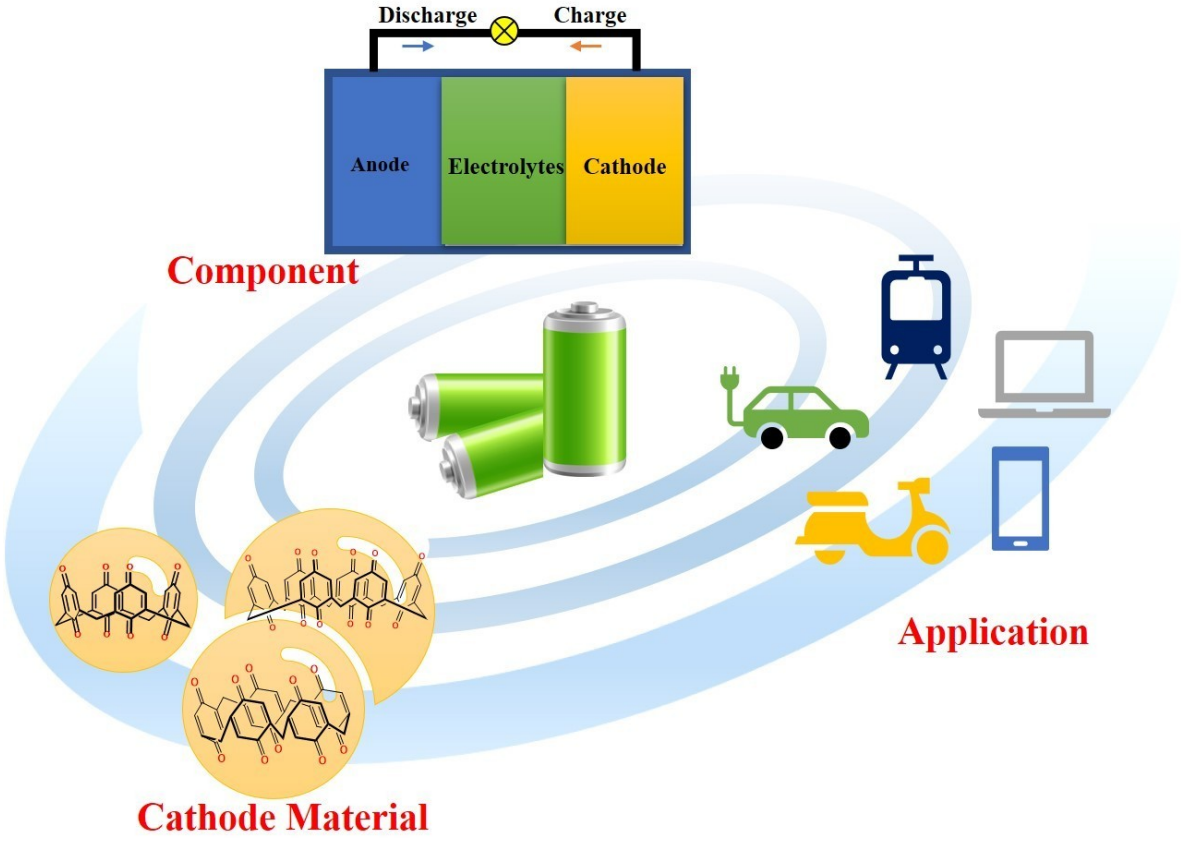

doi.org/10.1002/batt.202000038

Attributing to the advantages of high theoretical specific capacity, good structural designability and environmental friendliness, organic quinone electrode materials have been applied in secondary batteries to achieve great electrochemical performances. At present, a series of researches about secondary batteries with quinone-based compounds calix[4]quinone (C4Q), pillar[5]quinone (P5Q) and calix[6]quinone (C6Q) as cathodes have been carried out. In this review, we systematically summarize the applications of these three types of quinone compounds in lithium-ion batteries (LIBs), sodium-ion batteries (SIBs), zinc-ion batteries (ZIBs), and magnesium-ion batteries (Mg-ion batteries). The optimizing methods for suppressing the dissolution of organic electrode materials such as quasi-solid-state electrolytes, all-solid-state electrolytes, ionic liquid electrolytes, aqueous electrolytes and carbon immobilization are concluded. This review could provide a good guideline to improve the electrochemical performances of secondary batteries using quinone compounds as cathodes in the future.

1. Introduction

The continuous advancement in science and technology requires more efforts in the development of efficient and convenient energy storage devices. Since primary batteries can't be reused and normally contain heavy metals (*e.g.* mercury, cadmium, and lead) that can cause serious environmental pollution, it is highly desirable to develop eco-friendly secondary batteries that can be discharged and charged thousands of times. Clearly, these batteries are more economical and practical than primary batteries and have been widely used in various fields.[1]

Among all secondary batteries, lithium-ion batteries (LIBs), sodium-ion batteries (SIBs), and zinc-ion batteries (ZIBs) are currently the three most concerned types. Each of them has their own characteristics. On account of high energy density (generally above 120 $Wh\,kg^{-1}$), lightweight, small volume and wide operating temperature,[2] LIBs are widely used in mobile phones, computers, electric bicycles and other portable electronic devices. Generally, carbon materials, such as graphite ($C_{theo} = 372\ mAh\,g^{-1}$), are selected as anodes in LIBs, whose capacity is much higher than those of common inorganic cathode materials (*e.g.* $LiCoO_2$[3], $LiMn_2O_4$[4] and $LiFePO_4$[5]). In this situation, the capacities in both electrodes are not balanced and the relatively low capacity of inorganic cathode materials (around 140–170 $mAh\,g^{-1}$) will affect the actual reversible capacity and cycle performance of batteries.[6] Therefore, preparing suitable cathode materials plays the key role in improving the electrochemical performances of LIBs.[7]

In addition, the limited resources of lithium in nature has resulted in high production costs and further hinders the application of LIBs,[8] it is logical to switch to rich and cheap metal sources (*e.g.* Na, K, and Zn). It is well known that sodium resources are abundant, accounting for 2.64% of the crustal reserves (majority in seawater).[9] Sodium and lithium are in the same main group and have similar physicochemical properties. Thus, SIBs have the same electrochemical working principle to the rocking-chair LIBs. These mature working systems that have been researched in LIBs are the best references for SIBs.[10] Benefitted from the advantages mentioned above, SIBs have been studied extensively nowadays. It is worth noting that the large radius of Na^+ could slow down the speed of ions' intercalation/deintercalation in electrode materials, and affect the reversible capacity and rate performance.[11] Using disordered carbon anodes with large layer spacing rather than the graphite is the right choice in SIBs.[12]

To solve the capacity and cycle performance problems faced by LIBs and SIBs, the effective strategy is to prepare novel electrode materials with high specific capacity and select appropriate electrolytes. Limited by their specific capacity, it is difficult to make breakthroughs in inorganic electrode materials. Compared with inorganic electrode materials, the application of organic electrode materials or inorganic-organic hybrid materials can obtain better electrochemical benefits and effectively promote the development of secondary batteries.[13] First, the specific capacity of organic electrode materials is relatively high, making stronger competitiveness for organic rechargeable batteries. For example, poly(pyrene-4,5,9,10-tetraone) (PPTO) and poly(2,7-ethynylpyrene-4,5,9,10-tetraone) (PEPTO) have reversible capacities of 234 $mAh\,g^{-1}$ and 244 $mAh\,g^{-1}$, respectively.[14a] Yao *et al.* found that 2,5-dimethoxy-1,4-benzoquinone (DMBQ), as cathodes in LIBs, displayed the capacity of 312 $mAh\,g^{-1}$ in the first cycle, twice more than that of traditional cathode material $LiCoO_2$.[14b] Second, organic electrode materials have highly configurable structures so that the electrochemical redox properties can be adjusted by changing functional groups.[15] Third, organic compounds are usually composed of ordinary elements (C, H, O, N, P, S) and can be synthesized through different chemical reaction approaches.[16] Therefore, organic electrode materials have the advantages of abundant raw materials, low price and almost no resource limitation in the foreseeable future. Using organic materials instead of transition metal oxides as electrodes is less harmful to the environment and conforms to the green-sustainable development theory. Last, good structural stabilities and high thermal stabilities can help to extend cycle performance and safety of secondary batteries. However, two biggest issues existing in organic electrode materials are the dissolution in conventional organic electrolytes and poor conductivity.[17] Song *et al.* found that the initial capacity of anthraquinone in 1 M LiTFSI/DOL + DME electrolyte was 218 $mAh\,g^{-1}$ and de-

[a] *M. Zhang, Y. Zhang, Prof. W. Huang*
School of Environmental and Chemical Engineering
Yanshan University
Qinhuangdao 066004, China
E-mail: huangweiwei@ysu.edu.cn
[b] *Prof. W. Huang, Prof. Q. Zhang*
School of Materials Science and Engineering
Nanyang Technological University
50 Nanyang Avenue, 639798, Singapore Singapore
E-mail: QCZHANG@ntu.edu.sg

doi.org/10.1002/batt.202000038

creased rapidly from the second cycle. By introducing S–S bonds to form poly(anthraquinonyl sulfide), this system has higher utilization ratio and excellent cyclability.[18] Genorio *et al.* grafted the organic electrode material CQ onto the surface of insoluble substrate nano-silica particles for the first time, which provides the possibility to improve battery performance at the nano-level.[19] The polyimide/graphene composite organic cathodes with high conductivity prepared by Lyu *et al.* enabled a high capacity of 232.6 mAh g^{-1} and an excellent cycling stability.[20] Optimizing molecular structures, immobilizing active substances, developing solid electrolytes and adding conductive materials[21] are the common effective solutions to the above-mentioned two problems.

Considering the high solubility of organic electrodes in organic electrolytes and poor solubility in aqueous electrolytes, using aqueous electrolytes could solve the serious dissolution problem of organic electrode materials. The application of aqueous electrolytes can also avoid the security incidents caused by the flammability of conventional electrolytes and improve the safety performance of rechargeable batteries. The ionic conductivity of aqueous electrolytes is higher than that of organic electrolytes, which makes batteries possess a higher power density.[22] Moreover, aqueous electrolytes have good compatibility with metal Zn, which has a lower redox potential ($Zn/Zn^{2+} = -0.76$ V). The high volumetric capacity, low cost and non-toxicity make the development and application of aqueous ZIBs particularly attractive. Shoji *et al.* first reported a rechargeable Zn-MnO_2 aqueous battery with aqueous $ZnSO_4$ electrolyte, which opens the door to the research of aqueous ZIBs.[23] At present, organic electrodes also have been used in ZIBs. For instance, tetrachloro-1,4-benzoquinone cathode in aqueous ZIBs proposed by Kundu *et al.* showed a high capacity of more than 200 mAh g^{-1}.[24] Guo *et al.* assembled aqueous ZIBs with 4,5,9,10-tetraone cathode in 2 M $ZnSO_4$ aqueous electrolyte, which produced an excellent capacity of 336 mAh g^{-1} at a current density of 0.04 A g^{-1}.[25] Obviously, organic electrodes could display excellent performances in aqueous ZIBs. Thus, exploring high-performance organic electrodes is of great significance in the future.

Organic electrode materials have a universal applicability in LIBs, SIBs and ZIBs, which also provides a possibility for their practical application in secondary batteries in the future. Currently, there are approximately four categories of organic electrode materials that have been studied: conductive polymers,[26] organic radical polymers,[27] organic sulfides,[28] and organic carbonyl compounds.[29] As a kind of organic carbonyl compounds, quinone compounds have excellent redox properties, which has attracted more researchers' attention.[30] Benzoquinone (BQ),[14,31] anthraquinone (AQ)[32] and naphthoquinone (NQ)[33] are the most typical and widely used organic quinone compounds in secondary batteries. These compounds contain large conjugated systems with multiple carbonyl functional groups, and have the advantages of high specific capacity, diverse structures and fast electrochemical reactions.[34] Electron transfer at the carbonyl sites is the key to the intercalation/deintercalation of ions. In the discharge process, the neutral carbonyl groups get electrons to form free radical oxygen anions, which can combine with metal ions to form salts; while

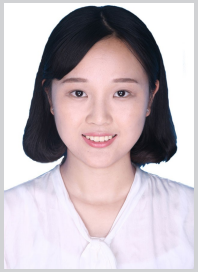

Meng Zhang received her B.S. in Applied Chemistry from Jiangxi Science and Technology Normal University in 2018. She is currently pursuing her Master's degree under the supervision of Prof. Weiwei Huang at Yanshan University. Her major research interests focus on the synthesis and preparation of organic cathode materials for Li/Na batteries.

Yi Zhang received her B.S from Hebei Normal University in 2019. Now she is a master student under the guidance of Prof. Weiwei Huang at Yanshan University. Her research mainly focuses on the synthesis and preparation of organic electrode materials in Li/Na batteries and investigation of electrolytes.

Weiwei Huang obtained her B.Sc. degree at Hebei Normal University of Science & Technology in 2005, M.Sc. degree of inorganic chemistry at Hebei Normal University in 2008, and Ph.D. degree of physical chemistry at Nankai University in 2011. Then, she joined Prof. Jun Chen's group at Nankai University as a postdoctoral fellow. Since 2013, she joined the School of Environmental and Chemical Engineering at Yanshan University as an associate professor. She was a visiting scholar at Nanyang Technological University in 2019. Her research is focused on the organic electrode materials for Li/Na batteries.

Qichun Zhang is an Associate Professor at the School of Materials Science and Engineering, Nanyang Technological University, Singapore. His research focuses on conjugated rich carbon materials and applications. Currently, he is an associate editor for J. Solid State Chemistry, Advisory board members of Materials Chemistry Frontiers, Chemistry - an Asian Journal, Journal of Materials Chemistry C, and Inorganic Chemistry Frontiers. He also is a fellow of the Royal Society of Chemistry. In 2018 and 2019, he has been recognized as one of highly cited researchers (top 1%) in cross-field in Clarivate Analytics. Till now, he has published more than 350 papers (H-index: 71) and 4 patents.

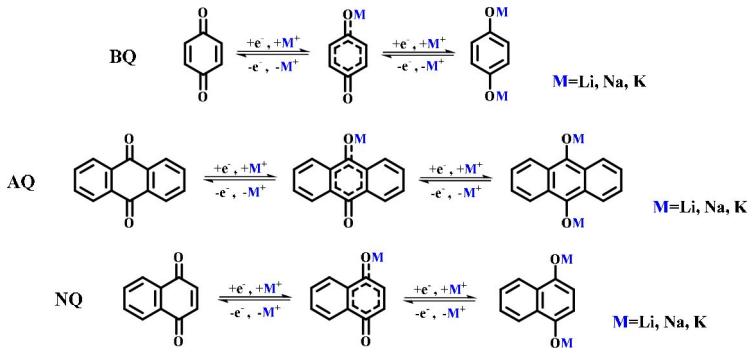

Figure 1. Reaction mechanism of quinone electrodes with monovalent metal ions.

during the charge process, the corresponding metal ions and electrons remove from the binding sites and the active sites are restored as the carbonyl structures (Figure 1). The redox mechanism, based on the break and formation of large conjugate π bonds on the carbonyl groups, is applicable to most metal ions, such as Li^+, Na^+, and K^+.[35]

Calix[4]quinone (C4Q, $C_{28}H_{16}O_8$), derived from calix[4]arene, basically retains its cup-shaped molecular structure. Consisting of four *p*-benzoquinone structures connected by methylene (–CH_2), C4Q could rotate in space and has small steric hindrance. With eight carbonyl groups, C4Q can provide eight intercalation/deintercalation sites for univalent metal ions during the electrochemical redox reaction. Similar to the structure of C4Q, pillar[5]quinone (P5Q, $C_{35}H_{20}O_{10}$) consists of five *p*-benzoquinone units and its para-position is linked by -CH_2 to form a macromolecular ring structure. The cavity radius of P5Q is 4.128 Å[36] and it also has a smaller steric hindrance and extremely high molecular symmetry. Compared with C4Q, the ten carbonyl units in P5Q would participate in the electrochemical reaction. Calix[6]quinone (C6Q, $C_{42}H_{24}O_{12}$) has the largest molecular weight and the most stable structure. All twelve carbonyl groups within this molecule can undergo reversible intercalation/deintercalation reactions of ions.

These quinone compounds (C4Q, P5Q and C6Q) have similar structures and electrochemical redox mechanisms. Taking C4Q as an example, its redox mechanism is shown in Figure 2. Although their molecular weights are different, these materials still have the same theoretical specific capacity ($C_{theo} = 446$ mAh g^{-1}), which is significantly higher than those of traditional inorganic electrode materials and common organic electrode materials. Through the density functional theory (DFT) calculation (Figure 3), it is more intuitive to see their

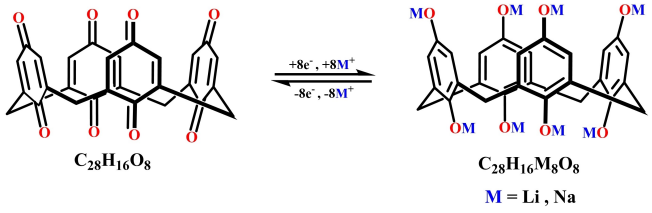

Figure 2. The redox reaction mechanisms of C4Q cathode materials.

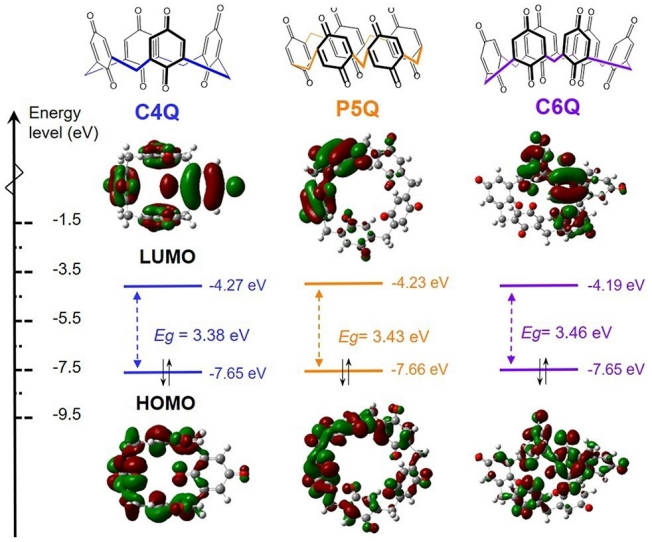

Figure 3. The energy diagrams of C4Q, P5Q and C6Q. Reproduced with permission.[37] Copyright 2019, Elsevier.

molecular structures and energy levels. The lowest unoccupied molecular orbital (LUMO) indicates that these molecules are strong electron acceptors, which have good electron affinity. The energy gaps (*E.g.*) between the highest occupied molecular orbital (HOMO) and LUMO represent different electron transfer difficulties. The *Egs* of C4Q, P5Q and C6Q are relatively small, which further demonstrates that these molecules have good application prospects when used as electrode materials.[37]

This review comprehensively describes the basic electrochemical properties of C4Q, P5Q and C6Q as cathodes in secondary batteries, and summarizes the methods mentioned in previous researches to effectively alleviate the dissolution rate of such quinone compounds in organic electrolytes. Hopefully, our review could provide basic ideas for future improving the properties of quinone-based organic electrode materials.

2. Applications in LIBs

According to the buckets effect, the capacity of cathode materials determines the overall electrochemical performance of LIBs. Figure 4 is the illustration of rechargeable LIBs using quinone electrodes. The theoretical specific capacities of C4Q, P5Q and C6Q are comparatively high, and their applications in LIBs display good electrochemical performances close to the theoretical capacity.

Our group conducted the electrochemical tests on conventional liquid LIBs with C4Q, P5Q, or C6Q as cathodes, lithium metal as anodes, and 1 M $LiPF_6$ ethylene carbonate (EC)/dimethyl carbonate (DMC) solution (v:v = 1:1) as electrolytes. The tests were operated by Zheng *et al.* at the current density of 0.1 C and a working voltage of 1.5–3.5 V.[38] The C4Q-LIBs exhibited an initial discharge capacity of 427 mAh g^{-1}, which is the 89.5% of the C_{theo} (446 mAh g^{-1}), however, the capacity dropped rapidly to 27.9 mAh g^{-1} at 50 cycles (Figure 9a). Later on, the P5Q-LIBs were tested by Zhu *et al.* at 0.2 C within 1.8–3.3 V.[39] The discharge and charge capacities in the first cycles were 405 mAh g^{-1} and 317 mAh g^{-1}, respectively. With cycles increasing, the capacity decreased rapidly to less than 100 mAh g^{-1} only in the fifth cycles (Figure 5a and 5b). Huang and Zhang *et al.* assembled LIBs with C6Q/ketjen black/polyvinylidene difluoride (PVDF) (6:3:1) electrode,[40] and this battery produced an initial discharge capacity of 423 mAh g^{-1}, reaching 95% of the C_{theo}. After 100 cycles, it decreased to 216 mAh g^{-1} at 0.1 C (Figure 9b).

The above-mentioned results indicate that, LIBs with C4Q, P5Q or C6Q as cathodes showed the initial discharge capacities close to the theoretical capacity, which proves that all their carbonyl sites would participate in electrochemical redox reactions. However, there still exists a rapid capacity decay problem during cycles when they are used as cathodes in liquid LIBs. The similarity compatibility principle can explain this problem reasonably. C4Q, P5Q and C6Q all belong to the family of organic carbonyl compounds, which easily dissolved in organic liquid electrolytes, leading to rapid capacity declines.

Converting organic liquid electrolytes into gel polymer electrolytes (GPE) to assemble quasi-solid-state batteries is one of the effective ways to address the dissolution issue.[41] Huang *et al.* prepared quasi-solid-state LIBs with a high-capacity organic cathode material C4Q in poly(methacrylate) (PMA)/poly (ethylene glycol) (PEG)-based GPE containing $LiClO_4$ in DMSO.[42] The as-fabricated battery showed 422 mAh g^{-1} at first cycles and remained at 379 mAh g^{-1} after 100 cycles at 0.2 C (Figure 6a). Since GPE could effectively improve the performance of LIBs with C4Q cathode, Zhu *et al.* conducted the quasi-solid-state LIBs with P5Q cathode.[39] The initial discharge capacity was increased to 410 mAh g^{-1}. After 100 cycles, the capacity was still 363 mAh g^{-1} at 0.2 C (Figure 6c and 6d). These results show that PMA/PEG GPE also matches well with P5Q, which is expected to be used with other organic cathode materials to build up the electrochemical properties of LIBs.

However, a small amount of liquid electrolyte is still required to be added into GPE during the preparation process, which maybe evaporate at high temperatures, resulting in a decrease in electrical conductivity. The composite polymer electrolytes (CPE), by contrast, have high fluidity, good solubility and more stable interfacial properties. Assembling all-solid-state batteries with CPE can better solve the dissolution problem.[43] Zhu *et al.* further prepared a novel PMA/PEG-$LiClO_4$-3 wt% SiO_2 CPE with an optimal ionic conductivity of 0.26 mS cm^{-1} at 25 °C.[44] The electrochemical performance of all-solid-state P5Q-LIBs with PMA/PEG-SiO_2 CPE is exhibited in

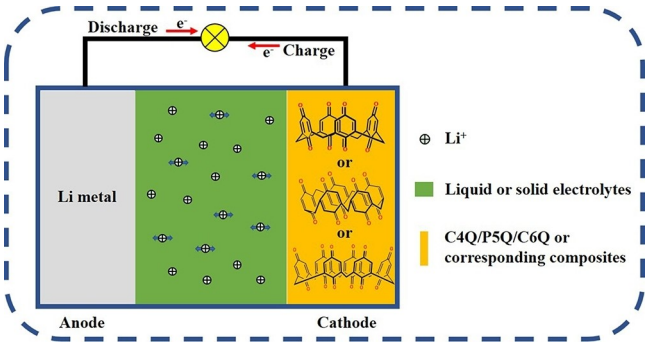

Figure 4. Illustration of rechargeable LIBs using quinone electrodes.

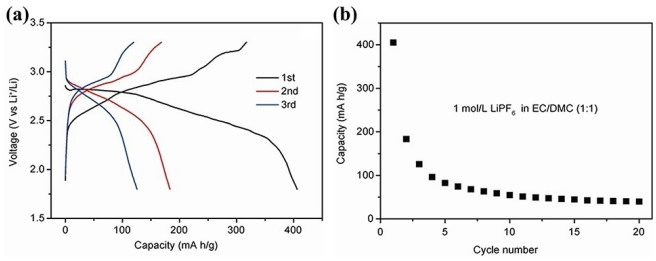

Figure 5. a) Discharge-charge curves and b) cycle performance of the liquid LIBs with P5Q as cathodes. Reproduced with permission.[39] Copyright 2014, Science China Press.

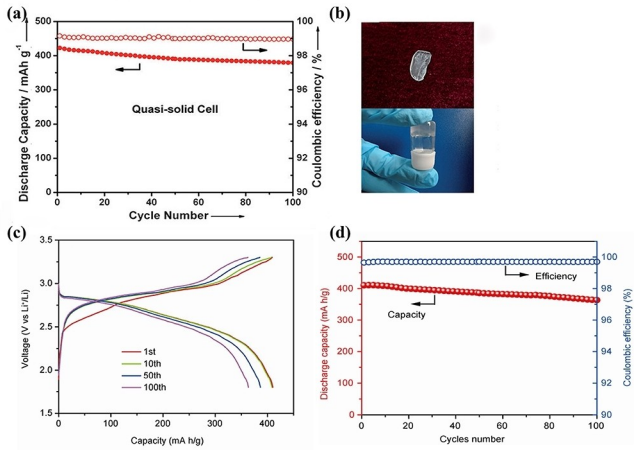

Figure 6. a) Cycle performance of quasi-solid-state C4Q-LIBs with PMA/PEG GPE. b) The pictures of PMA/PEG hybrid and PMA/PEG-based GPE loading $LiClO_4$ in DMSO. Reproduced with permission.[42] Copyright 2013, Wiley-VCH Verlag GmbH & Co. KGaA. c) Discharge-charge curves and d) cycle performance of quasi-solid-state batteries composed of P5Q and PMA/PEG GPE at 0.2 C. Reproduced with permission.[39] Copyright 2014, Science China Press.

Figure 7. The initial discharge capacity was 418 mAh g^{-1} and the average operating voltage was 2.6 V. After 50 cycles, the capacity maintained 94.7% of the first cycle (0.2 C), while at 0.3 C, 0.5 C and 1 C, the capacities were still 361, 286 and 197 mAh g^{-1}, respectively.

In a recent study, Huang and Zheng *et al.* fundamentally explored the changes of carbonyl sites in C6Q during discharge-charge progress by in-situ infrared spectroscopy (IR).[37] It is clear that the vibration peak (1650 cm^{-1}) of carbonyl groups decreased with the discharging progress and increased continuously when charging (Figure 8a), which better proves the redox reversibility of C6Q. The excellent solvating capability and penetrability of plastic crystal electrolyte (PCE) provide the possibility to further reduce the interface resistance and volume change while cycling. The PCE with succinonitrile (SN) as matrix and different concentrations of $LiClO_4$ and LiTFSI as dopants salt were prepared. Among these samples, only the 5 mol% LiTFSI/SN system meets the requirements of solid-state electrolytes. The assembled C6Q-PCE all-solid-state LIBs (using 5 mol% of LiTFSI in SN) revealed a discharge specific capacity of 425 mAh g^{-1} at the first cycle (0.05 C) and retained 405 mAh g^{-1} after 500 cycles at 0.1 C. It is worth noting that the replacement of traditional organic liquid electrolytes with polymer electrolytes can not only slow down the dissolution rate of cathode materials and increase the transmission rate of Li^+ in electrolytes, but also improve the safety of batteries. The development of solid-state secondary batteries possesses a promising prospect.

Using porous carbon materials to immobilize active substances to avoid direct contact with organic electrolytes is another common method to suppress the dissolution and thereby improve the electrochemical performance of active materials. Zheng *et al.* chose ordered mesoporous carbon CMK-3 to immobilize C4Q and prepared C4Q/CMK-3 composites with different components by ultrasonic perfusion.[38] According to Figure 9a, the C4Q/CMK-3 (1:2) composite realized a high discharge capacity of 427 mAh g^{-1} and kept 251.2 mAh g^{-1} at 100 cycles (0.1 C). The same method was chosen for the modification of C6Q.[40] It can be seen from Figures 9b and 9c that the C6Q/CMK-3 (1:2) composite has the highest capacity, best rate capability and cycle stability, and it maintained 273 mAh g^{-1} after 300 cycles at 0.1 C. The preparation of composites alleviates the dissolution rate of active materials to some extent and improves the performance of batteries. However, the mass ratio of CMK-3 is relatively high, accounting for 40% of the whole electrode, which is not conducive to

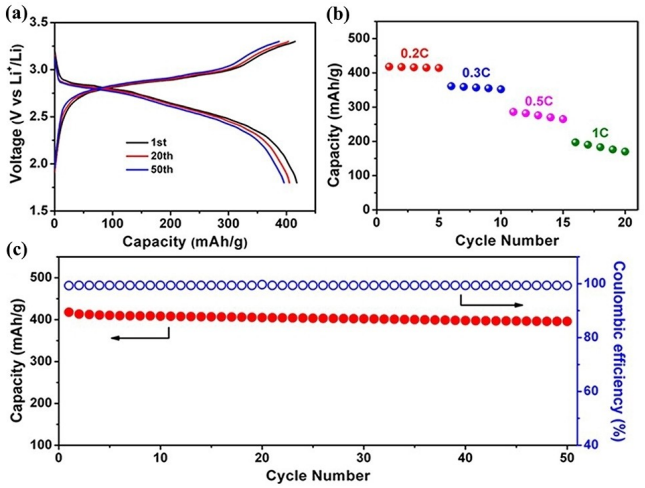

Figure 7. Electrochemical performances of all-solid-state P5Q-LIBs with PMA/PEG-$LiClO_4$-3 wt% SiO_2 CPE: a) discharge-charge curves, b) rate capability and c) cycle performance between 1.8 V and 3.3 V at 0.2 C. Reproduced with permission.[44] Copyright 2014, American Chemical Society.

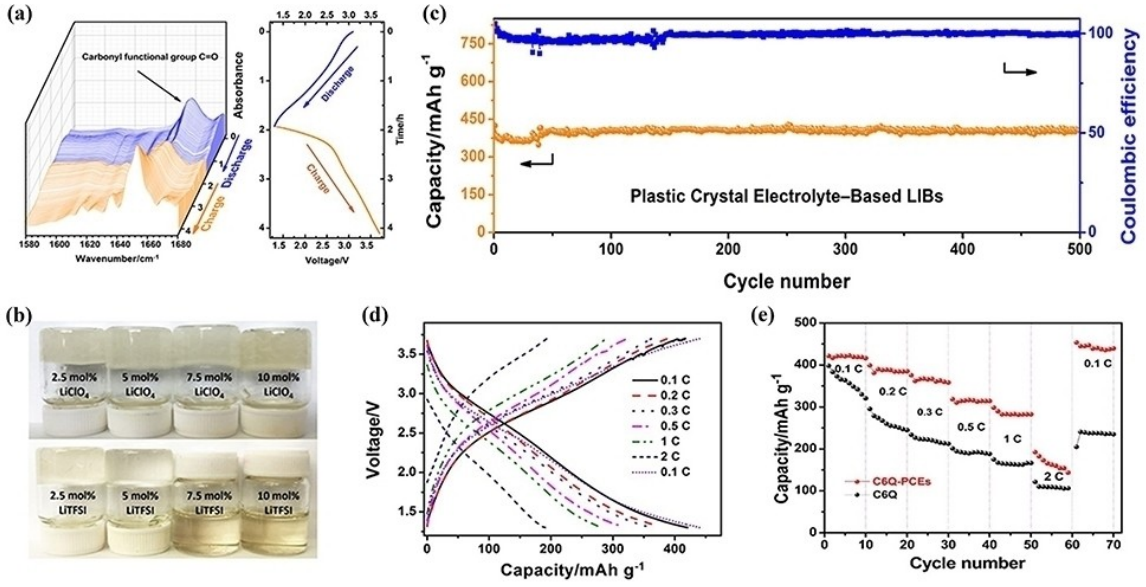

Figure 8. a) In-situ IR spectra of C6Q cathode. b) The comparison pictures of PCE with different $LiClO_4$ and LiTFSI components. c) Cycle performance of PCE-based LIBs with C6Q cathode. d) Discharge-charge curves at different current densities and e) rate performances of C6Q PCE-based LIBs. Reproduced with permission.[37] Copyright 2019, Elsevier.

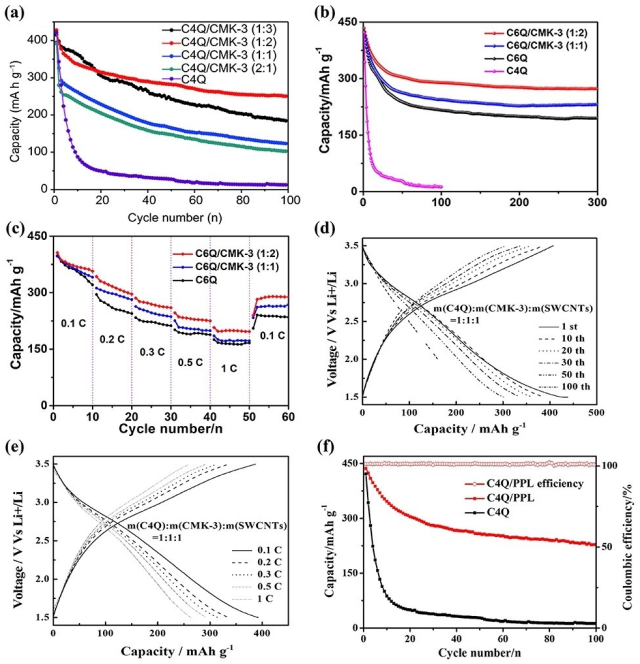

Figure 9. a) Cycle performances of C4Q and different C4Q/CMK-3 composites. Reproduced with permission.[38] Copyright 2018, Springer Nature. b) Cycle performances and (c) rate capability of C6Q and its composites. Reproduced with permission.[40] Copyright 2019, Springer Nature. d) Discharge-charge curves of C4Q/CMK-3/SWCNTs composite at 0.1 C and e) their discharge-charge curves at different current densities. Reproduced with permission.[45] Copyright 2019, Chinese Journal of Applied Chemistry. f) Cycle performances of C4Q/PPL composite. Reproduced with permission.[46] Copyright 2019, Wiley-VCH Verlag GmbH & Co. KGaA.

improving the energy density of rechargeable batteries. By adding single-walled carbon nanotubes (SWCNTs) to C4Q/CMK-3 composite, Yan *et al.* constructed a three-dimensional conductive network (C4Q/CMK-3/SWCNTs).[45] It can reduce the use of CMK-3 and promote the conductivity of cathode materials. The initial capacity of C4Q/CMK-3/SWCNTs (mass ratio, 1:1:1) was 438 mAh g^{-1} and remained at 238.7 mAh g^{-1} after 100 cycles. When the current density increased to 1 C, the discharge capacity was still 260 mAh g^{-1} (Figure 9d and 9e). Taking the high costs of CMK-3 and SWCNTs into consideration when practical applying, Huang and Zhang *et al.* prepared a novel cost-effective biomass carbon material PPL from calyxes of Physalis Peruviana L.[46] The LIBs with C4Q/PPL cathode displayed an initial capacity of 437 mAh g^{-1} and maintained 228 mAh g^{-1} after 100 cycles when the current density was 0.1 C (Figure 9f).

The above-mentioned researches verify the universal adaptability of quinone compounds C4Q, P5Q and C6Q as organic cathode materials in rechargeable LIBs. All datum of LIBs involved in these researches are summarized in Table 1. With the continuous increase of molecular weight, the dissolution rate in traditional liquid electrolytes decreases gradually, the cycle performance tends to be stable, and the capacity decreases slowly. Moreover, both solid electrolytes and porous carbon materials can be used to modify the organic cathode materials for improving the cycling stability.

3. Applications in SIBs

Since C4Q, P5Q and C6Q have already shown the outstanding electrochemical performance when used as cathode materials in LIBs, it is reasonable to extend these researches in SIBs. Liquid SIBs can be assembled with C4Q or P5Q as the cathode, Na metal as the anode, and 1 M $NaClO_4$ in EC/DMC (v:v = 1:1) containing 5% fluoroethylene carbonate (FEC) as electrolytes. Zheng *et al.* investigated the electrochemical performance of C4Q-based liquid SIBs,[47] whose initial discharge capacity (440 mAh g^{-1}) was better than that in LIBs at 0.1 C, but the dissolution problem of C4Q was worse and the capacity reduced to 24 mAh g^{-1} at 10th cycles (Figure 11a). Xiong *et al.* tested the electrochemical performance of P5Q-SIBs.[48] From Figure 11d, the discharge capacity was 431 mAh g^{-1} and decreased to 117 mAh g^{-1} (retention rate is 27%) after 100 cycles. Because the dissolution problem is an intrinsic property of organic electrode materials, it does not disappear even after the battery type changes. Thus, there is no doubt that the solubility issue still exists in SIBs, which might be the dominant factor of the decrease in cycle stability.

The usage of ionic liquid electrolytes is considered as an effective method for the preparation of high-energy and long-cycle SIBs. Ionic liquid electrolytes have inhibitory effects on the dissolution of quinone materials related to their strong polarity, weak electron donor capacity and low interaction energy.[49] In addition, compared with organic liquid electrolytes, ionic liquid electrolytes have the advantages of low flammability, high thermal stability and electrochemical stability, which may be ensured for the safety of secondary batteries when cycles. Wang *et al.* prepared six kinds of ionic liquids and assembled with C4Q electrode sheets (C4Q:conductive carbon:adhesive = 50:40:10) to form SIBs.[50] From Figure 10, it can be seen that SIBs with *N*-methyl-*N*-propylpyrrolidine bis(trifluoromethanesulfonyl)amide ([PY13][TFSI]) ionic liquid electrolytes performed better than others. It can not only solve the conundrum of quinone electrode materials dissolving in organic electrolytes, but also show a high capacity (> 400 mAh g^{-1}) and a superior capacity retention (still 99.7% after 300 cycles at a current density of 130 mA g^{-1}) when compared with ethylene glycol dimethyl ether (DME).

Compared to the preparation of ionic liquid electrolytes, using carbon materials to immobilize cathode materials is cheaper and simpler to be operated.[51] Zheng *et al.* applied C4Q/CMK-3 (1:2) composite to SIBs and found that the initial discharge capacity was up to 438 mAh g^{-1} and remained at 219.2 mAh g^{-1} after 50 cycles (Figure 11a).[47] These results demonstrate that immobilizing active materials by carbon materials also has excellent effects on enhancing the electrochemical properties of SIBs. In addition, the ternary composite C4Q/CMK-3/SWCNTs also can be applied to SIBs.[52] For the first cycle at 0.1 C, the capacity was 441 mAh g^{-1} and remained 75% after 50 cycles. The reversible capacity of 100 cycles was still 290 mAh g^{-1} and 66% of the retention rate (Figure 11b). Because CMK-3/SWCNTs is a relatively mature system, which displays the best performance in the rechargeable batteries, Xiong *et al.* directly chose CMK-3/SWCNTs system to immobilize

Table 1. Main parameters and electrochemical properties of LIBs with C4Q, P5Q and C6Q as cathodes.

LIBs	Electrode composition	Mass ratio	Electrolytes	Initial capacity [mAh g^{-1}]/ current density [C]	Reversible capacity [mAh g^{-1}]/ cycle number/ current density [C]	Capacity fading rate/ cycle number/ current density [C]	Ref.
C4Q	C4Q:Super P:PVDF	60:25:15	1 M $LiPF_6$ in EC/DMC (v:v=1:1)	427/0.1	27.9/50/0.1	93.5%/50/0.1	[38]
C4Q	C4Q:CMK-3: Super P:PVDF	27:53:5:15	1 M $LiPF_6$ in EC/DMC (v:v=1:1)	427/0.1	251.2/100/0.1	41.2%/100/0.1	[38]
C4Q	C4Q:CMK-3: SWCNTs:PVDF	30:30:30:10	1 M $LiPF_6$ in EC/DMC (v:v=1:1)	438/0.1	238.7/100/0.1	45.5%/100/0.1	[45]
C4Q	C4Q:PPL:PVDF	45:45:10	1 M $LiPF_6$ in EC/DMC (v:v=1:1)	437/0.1	228/100/0.1	47.8%/100/0.1	[46]
C4Q	C4Q:Porous carbon black spheres:SWCNTs:PVDF	62:30:3:5	PMA/PEG GPE	422/0.2	379/100/0.2	10.2%/100/0.2	[42]
P5Q	P5Q:Carbon black:PVDF	60:30:10	1 M $LiPF_6$ in EC/DMC (v:v=1:1)	405/0.2	<100/5/0.2	>75.3%/5/0.2	[39]
P5Q	P5Q:Carbon black:PVDF	60:30:10	PMA/PEG GPE	410/0.2	363/100/0.2	11.5%/100/0.2	[39]
P5Q	P5Q:Porous carbon black spheres:SWCNTs: Graphene:CPE:PVDF	55:25:3:2:10:5	PMA/PEG-$LiClO_4$-3 wt% SiO_2 CPE	418/0.2	396/50/0.2	5.3%//50/0.2	[44]
C6Q	C6Q:Ketjen black:PVDF	60:30:10	1 M $LiPF_6$ in EC/DMC (v:v=1:1)	423/0.1	216/100/0.1 195/300/0.1	48.9%/100/0.1 53.9%/300/0.1	[40]
C6Q	C6Q:CMK-3:Ketjen black:PVDF	20:40:30:10	1 M $LiPF_6$ in EC/DMC (v:v=1:1)	433.5/0.1	273/300/0.1	37.0%/300/0.1	[40]
C6Q	C6Q:Ketjen black:PVDF	30:60:10	5 mol% LiTFSI/SN	425/0.05	405/500/0.1	–	[37]

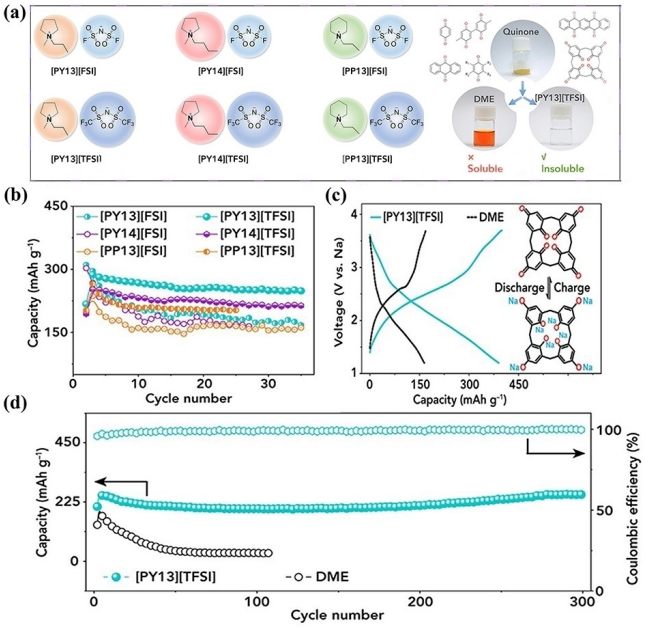

Figure 10. a) Structures and properties of ionic liquids. b) Cycle performances of C4Q cathode in six ionic liquid electrolytes at 0.2 C. c) Discharge-charge curves of C4Q in 0.3 M Na[TFSI]/DME and 0.3 M Na[TFSI]/[PY13][TFSI] ionic liquid electrolytes at 0.04 C and d) cycle performances of C4Q in above two kinds of electrolytes at 0.29 C. Reproduced with permission.[50] Copyright 2019, Elsevier.

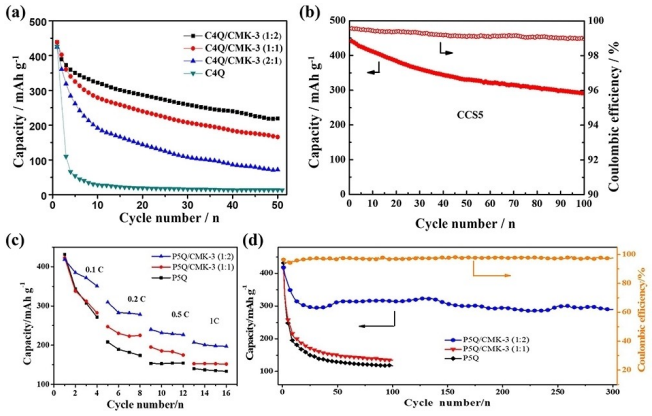

Figure 11. a) Cycle performances of C4Q and C4Q/CMK-3 (1:2) composite.[47] Reproduced by permission of The Royal Society of Chemistry. b) Cycle performance of C4Q/CMK-3/SWCNTs composite.[52] Reproduced by permission of The Royal Society of Chemistry. c) Rate capability and d) cycle performances of P5Q and P5Q/CMK-3 composite at 0.1 C. Reproduced with permission.[48] Copyright 2019, American Chemical Society.

P5Q in rechargeable SIBs.[48] Electrochemical tests were conducted on different P5Q/CMK-3 composite electrodes under the same condition. From Figure 11c and 11d, we can conclude that P5Q/CMK-3 (1:2) composite electrode has the best performances. The initial capacity reached 418 mAh g^{-1} and decreased to 290 mAh g^{-1} after 300 cycles at 0.1 C. When the

Table 2. Main parameters and electrochemical properties of SIBs with C4Q and P5Q as cathodes.

SIBs	Electrode composition	Mass ratio	Electrolytes	Initial capacity [mAh g^{-1}]/ current density [C]	Reversible capacity [mAh g^{-1}]/ cycle number/ current density [C]	Capacity fading rate/ cycle number/ current density [C]	Ref.
C4Q	C4Q:Super P: PVDF	60:25:15	1 M $NaClO_4$ in EC/DMC (v:v = 1:1) with 5% FEC	440/0.1	24/10/0.1	94.5%/10/0.1	[47]
C4Q	C4Q:CMK-3: Super P:PVDF	27:53:5:15	1 M $NaClO_4$ in EC/DMC (v:v = 1:1) with 5% FEC	438/0.1	219.2/50/0.1	50.0%/50/0.1	[47]
C4Q	C4Q:CMK-3: SWCNTs:PVDF	40:40:10:10	1 M $NaClO_4$ in EC/DMC (v:v = 1:1) with 5% FEC	441/0.1	290/100/0.1	34.2%/100/0.1	[52]
C4Q	C4Q:Conductive carbon:Adhesive	50:40:10	0.3 M Na[TFSI]/ [PY13][TFSI]	–	406/10/0.04	–	[50]
P5Q	P5Q:SWCNTs: PVDF	30:60:10	1 M $NaClO_4$ in EC/DMC (v:v = 1:1) with 5% FEC	431/0.2	117/100/0.2	72.9%/100 /0.2	[48]
P5Q	P5Q:CMK-3: SWCNTs:PVDF	20:40:30:10	1 M $NaClO_4$ in EC/DMC (v:v = 1:1) with 5% FEC	418/0.1	290/300/0.1	30.6%/300/0.1	[48]

current density increased to 1 C, it still maintained 201 mAh g^{-1}. Table 2 shows the main parameters and electrochemical properties of SIBs with C4Q and P5Q as cathodes.

4. Applications in Aqueous ZIBs and Mg–Ion Batteries

Aqueous ZIBs have attracted the attention of many scientists because aqueous electrolytes are less expensive and much safer in cycle process as well as the rich amount and low price of Zinc.[53] Since quinone materials are almost insoluble in water, it is envisaged as positive electrodes in aqueous ZIBs to obtain stable electrochemical performances.[54] Compared with inorganic electrodes, quinone compounds have larger capacities. The capacity and discharge-charge voltage vary with the location of the carbonyl group in quinone compounds. The steric resistance caused by the carbonyls in para-position for the movement of Zn^{2+} is small, thus quinone compounds with the para-position carbonyls usually have higher capacity and lower discharge-charge potential difference in general (Figure 12a). According to the theoretical calculations shown in Figure 12b, C4Q has lower LUMO energy and higher average discharge voltage.[55] Therefore, using C4Q as cathodes in aqueous ZIBs will maximize the possibility of obtaining excellent electrochemical performances.

Zhao *et al.* used C4Q as cathodes to turn this assumption into reality.[55] Different from the electrochemical redox mechanism of monovalent metal ions in LIBs, the eight carbonyl units of C4Q in ZIBs only provide six active sites for three Zn^{2+} to intercalate/deintercalate, and the remaining two distant

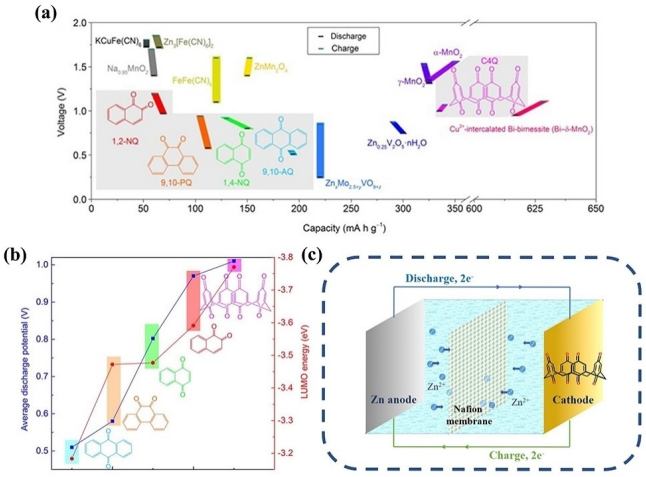

Figure 12. a) The comparison of discharge-charge voltages and capacities between several organic quinone electrodes and inorganic electrodes in aqueous ZIBs. b) LUMO energy and average discharge potential of different quinone compounds. Reproduced with permission.[55] Copyright 2018, American Association for the Advancement of Science. c) Illustration of aqueous ZIBs using C4Q cathode.

carbonyl groups are not involved in the reaction (Figure 13a). The aqueous C4Q-ZIBs revealed a high capacity of 335 mAh g^{-1}, so that C4Q is considered as one of the best cathode materials in ZIBs. The energy efficiency of ZIBs with C4Q was as high as 93% of initial capacity when the discharge-charge voltage gap was only 70 mA (Figure 13b). Since the discharge product Zn_xC4Q could dissociate into Zn^{2+} and $C4Q^{2-}$, the dissolved $C4Q^{2-}$ could pass through the film and react with the Zn anode to form by-products, affecting the electrochemical performance of ZIBs. To further reduce the capacity loss caused by the

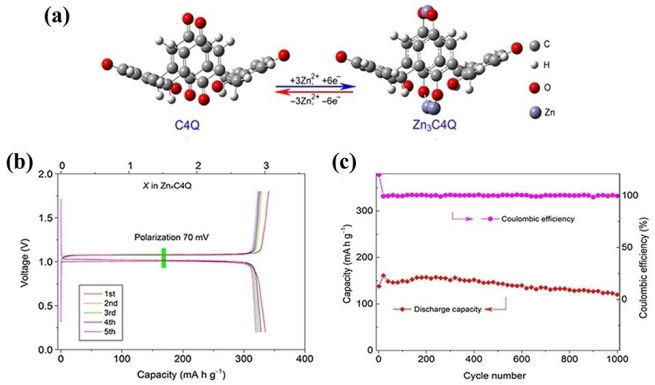

Figure 13. a) Electrochemical redox mechanism of C4Q in aqueous ZIBs. b) Discharge-charge curves of aqueous ZIBs with C4Q cathode at 20 mA g^{-1}. c) Cycle performance and coulombic efficiency of aqueous C4Q-ZIBs with Nafion separator at 500 mA g^{-1}. Reproduced with permission.[55] Copyright 2018, American Association for the Advancement of Science.

formation of by-products and dissolution of discharge products, the cation-selective Nafion membrane was used instead of conventional membranes in aqueous ZIBs with C4Q as cathodes. In Figure 13c, after 1000 cycles at the current density of 500 mA g^{-1}, the capacity maintained at 87% and decayed only 0.015% per revolution.

Moreover, Zhao *et al.* reported the application of C4Q as cathodes in Mg-ion secondary batteries with Mg as anode and

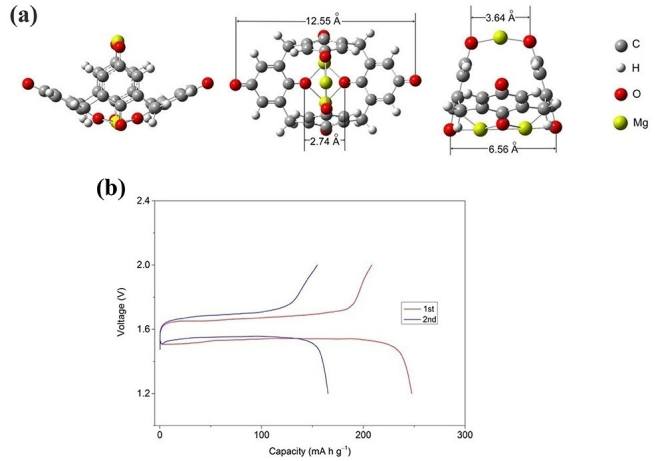

Figure 14. a) Structures of C4Q after uptake of three Mg^{2+}. b) Electrochemical performance of aqueous Mg–C4Q batteries. Reproduced with permission.[55] Copyright 2018, American Association for the Advancement of Science.

$Mg(CF_3SO_3)_2$ aqueous solution as electrolytes. Similar to the electrochemical mechanism of ZIBs, C4Q can only uptake three Mg^{2+} when applied in Mg-ion batteries. The experimental results showed that Mg-ion batteries with C4Q cathode presented an initial specific discharge capacity of 247.4 mAh g^{-1} at 20 mA g^{-1} and the discharge potential was 1.54 V (Figure 14b). Because of the slow kinetics of magnesium metal in aqueous electrolytes, the researches of quinone compounds in Mg-ion batteries are still rare, and the electrochemical performances of aqueous Mg-ion batteries need to be further improved. The performances of C4Q in aqueous ZIBs and Mg-ion batteries are summarized in Table 3.

Various optimization methods summarized in this review can be roughly divided into two categories: electrode modification and electrolyte modification. Designing new electrode materials with intrinsic insolubility or low solubility, increasing the molecular mass, and using porous carbon materials for immobilization are all viewed from the point of electrode modification, while electrolyte modification includes the preparation of various electrolytes (GPE, CPE, PCE) as well as the application of ionic liquid electrolytes and aqueous electrolytes. These two strategies could help improving the electrochemical performances of rechargeable batteries by reducing the dissolution of active substances and can be used as desirable guidelines in future researches.

5. Conclusions

We have reviewed the recent progress of quinone-based compounds (C4Q, P5Q and C6Q) as promising cathode materials in rechargeable LIBs, SIBs, aqueous ZIBs and Mg-ion batteries. In these batteries, all these materials displayed excellent electrochemical properties. Different strategies to address their dissolution issues in conventional liquid electrolytes and improve their electrochemical performances are also discussed. Using porous carbon materials to immobilize active substances can effectively avoid direct contact with electrolytes and slow down the dissolution rate of active substances. Moreover, modifying traditional liquid electrolytes to quasi-solid-state electrolytes and all-solid-state electrolytes, employing ionic liquid electrolytes, and switching to aqueous electrolytes are also effective methods to improve the cycle stability of secondary batteries. Our review would lighten the promising future of organic quinone electrode materials in secondary batteries.

Table 3. Main parameters and electrochemical properties of C4Q as cathodes in aqueous Zn/Mg secondary battery.

Battery	Separator	Electrode composition	Electrolytes	Initial capacity [mAh g^{-1}]/ current density [mA g^{-1}]	Capacity retention/ cycle number/ current density [mA g^{-1}]	Ref.
Zn	Nafion membrane	C4Q:Super P:PVDF	3 M $Zn(CF_3SO_3)_2$ aqueous solution	335/20	87%/1000/500	[55]
Mg	Porous filter paper	C4Q:Super P:PVDF	3 M $Mg(CF_3SO_3)_2$ aqueous solution	247.4/20	–	[55]

Acknowledgements

W.H. acknowledges the financial support of the National Natural Science Foundation of China (No. 21875206, 21403187) and the Natural Science Foundation of Hebei Province (No. B2019203487). Q.Z. acknowledges AcRF Tier 1 (Grants RG 111/17, RG 2/17, RG 114/16, RG 113/18) and Tier 2 (Grants MOE 2017-T2-1-021 and MOE 2018-T2-1-070), Singapore.

Conflict of Interest

The authors declare no conflict of interest.

Keywords: calix[4]quinone · calix[6]quinone · pillar[5]quinone · rechargeable batteries · organic electrodes

[1] a) M. Armand, J. M. Tarascon, *Nature* **2008**, *451*, 652–657; b) C. M. Park, J. H. Kim, H. Kim, H. J. Sohn, *Chem. Soc. Rev.* **2010**, *39*, 3115–3141; c) J. M. Tarascon, M. Armand, *Nature* **2001**, *414*, 359–367; d) F. Cheng, J. Liang, Z. Tao, J. Chen, *Adv. Mater.* **2011**, *23*, 1695–1715.
[2] a) J. B. Goodenough, K. S. Park, *J. Am. Chem. Soc.* **2013**, *135*, 1167–1176; b) A. G. Ritchie, *J. Power Sources* **2001**, *96*, 1–4; c) K. Kang, Y. S. Meng, J. Bre'ger, C. P. Grey, G. Ceder, *Science* **2006**, *311*, 977–980; d) B. Scrosati, J. Garche, *J. Power Sources* **2010**, *195*, 2419–2430.
[3] T. J. Boyle, D. Ingersoll, M. A. Rodriquez, C. J. Tafoya, D. H. Doughty, *J. Electrochem. Soc.* **1999**, *146*, 1683–1686.
[4] J. Tu, X. B. Zhao, D. G. Zhuang, G. S. Cao, T. J. Zhu, J. P. Tu, *Physica B* **2006**, *382*, 129–134.
[5] S. Yang, Y. Song, K. Ngala, P. Y. Zavalij, M. S. Whittingham, *J. Power Sources* **2003**, *119–121*, 239–246.
[6] a) S. Flandrois, B. Simon, *Carbon* **1999**, *37*, 165–180; b) Z. Li, G. Wu, D. Liu, W. Wu, B. Jiang, J. Zheng, Y. Li, J. Li, M. Wu, *J. Mater. Chem. A.* **2014**, *2*, 7471–7477; c) Y. Idota, T. Kubota, A. Matsufuji, Y. Maekawa, T. Miyasaka, *Science* **1997**, *276*, 1395–1397; d) K. T. Lee, J. C. Lytle, N. S. Ergang, S. M. Oh, A. Stein, *Adv. Funct. Mater.* **2005**, *15*, 547–556.
[7] E. Quartarone, P. Mustarelli, *Chem. Soc. Rev.* **2011**, *40*, 2525–2540.
[8] A. Manthiram, *JOM.* **1997**, *49*, 43–46.
[9] H. Li, C. Wu, F. Wu, Y. Bai, *Acta Chim. Sin.* **2014**, *72*, 21–29.
[10] a) S. W. Kim, D. H. Seo, X. Ma, G. Ceder, K. Kang, *Adv. Energy Mater.* **2012**, *2*, 710–721; b) V. Palomares, P. Serras, I. Villaluenga, K. B. Hueso, J. Carretero-González, T. Rojo, *Energy Environ. Sci.* **2012**, *5*, 5884–5901; c) S. Y. Hong, Y. Kim, Y. Park, A. Choi, N. S. Choi, K. T. Lee, *Energy Environ. Sci.* **2013**, *6*, 2067–2081.
[11] Q. Zhao, Y. Lu, J. Chen, *Adv. Energy Mater.* **2017**, *7*, 1601792.
[12] H. He, H. Wang, Y. Tang, Y. Liu, *Prog. Chem.* **2014**, *26*, 572–581.
[13] a) J. Xie, P. Gu, Q. Zhang, *ACS Energy Lett.* **2017**, *2*, 1985–1996; b) J. Xie, Q. Zhang, *J. Mater. Chem. A* **2016**, *4*, 7091–7106; c) J. Xie, C. Zhao, Z. Lin, P. Gu, Q. Zhang, *Chem. Asian J.* **2016**, *11*, 1489–1511; d) X. Zhan, Z. Chen, Q. Zhang, *J. Mater. Chem. A* **2017**, *5*, 14463–14479; e) Z. Wu, J. Xie, Z. Xu, S. Zhang, Q. Zhang, *J. Mater. Chem. A* **2019**, *7*, 4259–4290; f) J. Xie, Z. Wang, Z. J. Xu, Q. Zhang, *Adv. Energy Mater.* **2018**, *8*, 1703509; g) Z. Lin, J. Xie, B. Zhang, J. Li, J. Weng, R. Song, X. Huang, H. Zhang, H. Li, Y. Liu, Z. J. Xu, W. Huang, Q. Zhang, *Nano Energy* **2017**, *41*, 117–127; h) J. Xie, X. Cheng, X. Cao, J. He, W. Guo, D. Li, Z. J. Xu, Y. Huang, J. Lu, Q. Zhang, *Small* **2019**, *15*, 1903188; i) T. Sun, J. Xie, W. Guo, D. Li, Q. Zhang, *Adv. Energy Mater.* **2020**, DOI: 10.1002/aenm.201904199 .
[14] a) J. Xie, W. Chen, G. Long, W. Gao, Z. J. Xu, M. Liu, Q. Zhang, *J. Mater. Chem. A,* **2018**, *6,* 12985–12991; b) M. Yao, H. Senoh, S. I. Yamazaki, Z. Siroma, T. Sakai, K. Yasuda, *J. Power Sources* **2010**, *195*, 8336–8340.
[15] a) S. Goriparti, M. N. K. Harish, S. Sampath, *Chem. Commun.* **2013**, *49*, 7234–7236; b) R. Shi, L. Liu, Y. Lu, C. Wang, Y. Li, L. Li, Z. Yan, J. Chen, *Nat. Commun.* **2020**, *11*, 178.
[16] Y. Morita, S. Nishida, T. Murata, M. Moriguchi, A. Ueda, M. Satoh, K. Arifuku, K. Sato, T. Takui, *Nat. Mater.* **2011**, *10*, 947–951.
[17] a) Y. Ding, Y. Li, G. Yu, *Chem.* **2016**, *1*, 790–801; b) M. Miroshnikov, K. P. Divya, G. Babu, A. Meiyazhagan, L. M. R. Arava, P. M. Ajayan, G. John, *J. Mater. Chem. A* **2016**, *4*, 12370–12386.
[18] Z. Song, H. Zhan, Y. Zhou, *Chem. Commun.* **2009**, *4*, 448–450.
[19] B. Genorio, K. Pirnat, R. Cerc-Korosec, R. Dominko, M. Gaberscek, *Angew. Chem. Int. Ed.* **2010**, *49*, 7222–7224; *Angew. Chem.* **2010**, *122*, 7380–7382.
[20] H. L. Lyu, P. Li, J. Liu, S. Mahurin, J. Chen, D. K. Hensley, G. M. Veith, Z. Guo, S. Dai, X. Sun, *ChemSusChem* **2018**, *11*, 763–772.
[21] a) M. S. Whittingham, *Chem. Rev.* **2004**, *104*, 4271–4302; b) L. Zhao, W. Wang, A. Wang, K. Yuan, S. Chen, Y. Yang, *J. Power Sources* **2013**, *233*, 23–27; c) J. Xie, Z. Wang, P. Gu, Y. Zhao, Z. J. Xu, Q. Zhang, *Sci. China Mater.* **2016**, *59*, 6–11; d) J. Xie, W. Chen, Z. Wang, K. C. W. Jie, M. Liu, Q. Zhang, *Chem. Asian J.* **2017**, *12*, 868–876; e) C. Yao, Z. Wu, J. Xie, F. Yu, W. Guo, Z. J. Xu, D. Li, S. Zhang, Q. Zhang, *ChemSusChem* **2020**, DOI: 10.1002/cssc.201903007; f) C. Yao, J. Xie, Z. Wu, Z. J. Xu, S. Zhang, Q. Zhang, *Chem. Asian J.* **2019**, *14*, 2210–2214.
[22] a) W. Kaveevivitchai, A. Manthiram, *J. Mater. Chem. A* **2016**, *4*, 18737–18741; b) J. Xie, Q. Zhang, *Small* **2019**, *15*, 1805061; c) L. Chen, M. Yang, Z. Mei, L. Mai, *J. Inorg. Mater.* **2017**, *32*, 225–234.
[23] T. Shoji, M. Hishinuma, T. Yamamoto, *J. Appl. Electrochem.* **1988**, *18*, 521–526.
[24] D. Kundu, P. Oberholzer, C. Glaros, A. Bouzid, E. Tervoort, A. Pasquarello, M. Niederberger, *Chem. Mater.* **2018**, *30*, 3874–3881.
[25] Z. Guo, Y. Ma, X. Dong, J. Huang, Y. Wang, Y. Xia, *Angew. Chem. Int. Ed. Engl.* **2018**, *130*, 11911–11915.
[26] a) Z. Wang, N. Bramnik, S. Roy, G. Di Benedetto, J. L. Zunino, S. Mitra, *J. Power Sources* **2013**, *237*, 210–214; b) G. Milczarek, O. Inganas, *Science* **2012**, *335*, 1468–1471; c) P. Novák, K. Müller, K. S. V. Santhanam, O. Haas, *Chem. Rev.* **1997**, *97*, 207–282; d) L. Nyholm, G. Nyström, A. Mihranyan, M. Strømme, *Adv. Mater.* **2011**, *23*, 3751–3769.
[27] a) T. Suga, H. Nishide, *ACS Symp. Ser.* **2012**, *1096*, 45–53; b) I. S. Chae, M. Koyano, K. Oyaizu, H. Nishide, *J. Mater. Chem. A* **2013**, *1*, 1326–1333; c) K. Nakahara, S. Iwasa, M. Satoh, Y. Morioka, J. Iriyama, M. Suguro, E. Hasegawa, *Chem. Phys. Lett.* **2002**, *359*, 351–354; d) H. Nishide, S. Iwasa, Y. Pu, T. Suga, K. Nakahara, M. Satoh, *Electrochim. Acta* **2004**, *50*, 827–831.
[28] a) T. B. B. Dan, T. Frevert, B. Cavari, *Water Res.* **1985**, *19*, 983–985; b) Y. NuLi, Z. Guo, H. Liu, J. Yang, *Electrochem. Commun.* **2007**, *9*, 1913–1917; c) S. J. Visco, C. C. Mailhe, L. C. D. Jonghe, M. B. Armand, *J. Electrochem. Soc.* **1989**, *136*, 661–664.
[29] Z. Song, H. Zhou, *Energy Environ. Sci.* **2013**, *6*, 2280–2301.
[30] a) Z. Yao, W. Wei, J. Wang, J. Yang, Y. N. Nuli, *Acta Phys.-Chim. Sin.* **2011**, *27*, 1005–1016; b) B. Häupler, A. Wild, U. S. Schubert, *Adv. Energy Mater.* **2015**, *5*, 1402034; c) Y. Lu, Q. Zhang, L. Li, Z. Niu, J. Chen, *Chem.* **2018**, *4*, 1–28; d) Y. Lu, J. Chen, *Nat. Rev. Chem.* **2020**, *4*, 127–142.
[31] T. L. Gall, K. H. Reiman, M. C. Grossel, J. R. Owen, *J. Power Sources* **2003**, *119–121*, 316–320.
[32] a) Z. Song, H. Zhan, Y. Zhou, *Chem. Commun.* **2009**, *4*, 448–450; b) J. Bitenc, K. Pirnat, T. Bančič, M. Gaberšček, B. Genorio, A. Randon-Vitanova, R. Dominko, *ChemSusChem* **2015**, *8*, 4128–4132; c) W. Xu, A. Read, P. K. Koech, D. Hu, C. Wang, J. Xiao, A. B. Padmaperuma, G. L. Graff, J. Liu, J. Zhang, *J. Mater. Chem.* **2012**, *22*, 4032–4039.
[33] a) J. Lee, H. Kim, M. J. Park, *Chem. Mater.* **2016**, *28*, 2408–2416; b) M. Yao, T. Numoto, M. Araki, H. Ando, H. T. Takeshita, T. Kiyobayashi, *Energy Procedia* **2014**, *56*, 228–236; c) H. Li, W. Duan, Q. Zhao, F. Cheng, J. Liang, J. Chen, *Inorg. Chem. Front.* **2014**, *1*, 193–199.
[34] a) H. Alt, H. Binder, A. Köhling, G. Sandstede, *Electrochim. Acta* **1972**, *17*, 873–887; b) Y. Lu, X. Hou, L. Miao, L. Li, R. Shi, L. Liu, J. Chen, *Angew. Chem. Int. Ed.* **2019**, *58*, 7020–7024.
[35] a) G. Dawut, Y. Lu, Q. Zhao, J. Liang, Z. Tao, J. Chen, *Acta Phys.-Chim. Sin.* **2016**, *32*, 1593–1603; b) X. Xiang, Z. Kai, J. Chen, *Adv. Mater.* **2015**, *27*, 5343–5364.
[36] K. U. Lao, C. H. Yu, *J. Comput. Chem.* **2011**, *32*, 2716–2726.
[37] W. Huang, S. Zheng, X. Zhang, W. Zhou, W. Xiong, J. Chen, *Energy Storage Mater.* **2020**, *26*, 465–471.
[38] S. Zheng, H. Sun, B. Yan, J. Hu, W. Huang, *Sci. China Mater.* **2018**, *61*, 1285–1290.
[39] Z. Zhu, D. Guo, Z. Tao, J. Chen, *Sci. Sin. Chim.* **2014**, *44*, 1175–1180.
[40] W. Huang, X. Zhang, S. Zheng, W. Zhou, J. Xie, Z. Yang, Q. Zhang, *Sci. China Mater.* **2020**, *63*, 339–346.
[41] a) P. Wang, S. M. Zakeeruddin, J. E. Moser, M. K. Nazeeruddin, T. Sekiguchi, M. Grätzel, *Nat. Mater.* **2003**, *2*, 402–407; b) G. Pistoia, A. Antonini, G. Wang, *J. Power Sources* **1996**, *58*, 139–144; c) T. Zuo, Y. Shi,

X. Wu, P. Wang, S. Wang, Y. Yin, W. Wang, Q. Ma, X. Zeng, H. Ye, R. Wen, Y. Guo, *ACS Appl. Mater. Interfaces* **2018**, *10*, 30065–30070.
[42] W. Huang, Z. Zhu, L. Wang, S. Wang, H. Li, Z. Tao, J. Shi, L. Guan, J. Chen, *Angew. Chem. Int. Ed.* **2013**, *52*, 9162–9166; *Angew. Chem.* **2013**, *125*, 9332–9336.
[43] a) A. Hayashi, K. Minami, M. Tatsumisago, *J. Solid State Electrochem.* **2010**, *14*, 1761–1767; b) Y. S. Lee, J. H. Lee, J. A. Choi, W. Y. Yoon, D. W. Kim, *Adv. Funct. Mater.* **2012**, *23*, 1019–1027; c) A. M. Stephan, K. S. Nahm, *Polymer* **2006**, *47*, 5952–5964; d) E. Quartarone, P. Mustarelli, A. Magistris, *Solid State Ionics* **1998**, *110*, 1–14.
[44] Z. Zhu, M. Hong, D. Guo, J. Shi, Z. Tao, J. Chen, *J. Am. Chem. Soc.* **2014**, *136*, 16461–16464.
[45] B. Yan, W. Xiong, S. Zheng, X. Zhang, W. Huang, *Chinese J. Appl. Chem.* **2019**, *36*, 554–563.
[46] W. Huang, M. Zhang, H. Cui, B. Yan, Y. Liu, Q. Zhang, *Chem. Asian J.* **2019**, *14*, 4164–4168.
[47] S. Zheng, J. Hu, W. Huang, *Inorg. Chem. Front.* **2017**, *4*, 1806–1812.
[48] W. Xiong, W. Huang, M. Zhang, P. Hu, H. Cui, Q. Zhang, *Chem. Mater.* **2019**, *31*, 8069–8075.
[49] a) M. S. Islam, C. A. J. Fisher, *Chem. Soc. Rev.* **2014**, *43*, 185–204; b) A. Unemoto, H. Ogawa, Y. Gambe, I. Honma, *Electrochim. Acta* **2014**, *125*, 386–394.
[50] X. Wang, Z. Shang, A. Yang, Q. Zhang, F. Cheng, D. Jia, J. Chen, *Chem.* **2019**, *5*, 364–375.
[51] A. Jaffe, A. Saldivar Valdes, H. I. Karunadasa, *Chem. Mater.* **2015**, *27*, 3568–3571.
[52] B. Yan, L. Wang, W. Huang, S. Zheng, P. Hu, Y. Du, *Inorg. Chem. Front.* **2019**, *6*,1977–1985.
[53] X. Dong, H. Yu, Y. Ma, J. L. Bao, D. G. Truhlar, Y. Wang, Y. Xia, *Chem. Eur. J.* **2017**, *23*, 2560–2565.
[54] Y. Liang, Y. Jing, S. Gheytani, K. Y. Lee, P. Liu, A. Facchetti, Y. Yao, *Nat. Mater.* **2017**, *16*, 841–848.
[55] Q. Zhao, W. Huang, Z. Luo, L. Liu, Y. Lu, Y. Li, L. Li, J. Hu, H. Ma, J. Chen, *Sci. Adv.* **2018**, *4*, 1761.

Manuscript received: February 21, 2020
Revised manuscript received: March 19, 2020
Accepted manuscript online: March 20, 2020
Version of record online: April 3, 2020